

Search for an invisible vector boson from π^0 decays at NA62

Elisa Minucci* for the NA62 Collaboration†

INFN Laboratori Nazionali di Frascati, Italy

E-mail: elisa.minucci@cern.ch

The search for an invisible vector boson from π^0 decays at the NA62 experiment at CERN Super Proton Synchrotron (SPS) is discussed. Within the proposed models for physics beyond the SM, hidden sectors consisting of new, light, weakly-coupled particles are a particularly compelling possibility. Thanks to the high beam intensity, the extremely good performance of the photon detection systems, particle identification system and the detectors timing, NA62 is suited to search for these new particles. Here the search for a dark photon from π^0 decays using the $K^+ \rightarrow \pi^+ \pi^0$, $\pi^0 \rightarrow A' \gamma$ decay chain is illustrated. The result from the analysis of a sub-sample of 2016 data is reported, corresponding to 1% of the full statistics collected in 2016-2018. A new upper limit on the $\pi^0 \rightarrow A' \gamma$ branching ratio has been set as a function of the dark photon mass, thus producing a new upper limit on the dark photon coupling parameter [1].

European Physical Society Conference on High Energy Physics - EPS-HEP2019 -
10-17 July, 2019
Ghent, Belgium

*Speaker.

†R. Aliberti, F. Ambrosino, R. Ammendola, B. Angelucci, A. Antonelli, G. Anzivino, R. Arcidiacono, T. Bache, M. Barbanera, J. Bernhard, A. Biagioni, L. Bician, C. Biino, A. Bizzeti, T. Blazek, B. Bloch-Devaux, V. Bonaiuto, M. Boretto, M. Bragadireanu, D. Britton, F. Brizioli, M.B. Brunetti, D. Bryman, F. Bucci, T. Capussela, J. Carmignani, A. Ceccucci, P. Cenci, V. Cerny, C. Cerri, B. Checcucci, A. Conovaloff, P. Cooper, E. Cortina Gil, M. Corvino, F. Costantini, A. Cotta Ramusino, D. Coward, G. D'Agostini, J. Dainton, P. Dalpiaz, H. Danielsson, N. De Simone, D. Di Filippo, L. Di Lella, N. Doble, B. Dobrich, F. Duval, V. Duk, J. Engelfried, T. Enik, N. Estrada-Tristan, V. Falaleev, R. Fantechi, V. Fascianelli, L. Federici, S. Fedotov, A. Filippi, M. Fiorini, J. Fry, J. Fu, A. Fucci, L. Fulton, E. Gamberini, L. Gatignon, G. Georgiev, S. Ghinescu, A. Gianoli, M. Giorgi, S. Giudici, F. Gonnella, E. Goudzovski, C. Graham, R. Guida, E. Gushchin, F. Hahn, H. Heath, E.B. Holzer, T. Husek, O. Hutanu, D. Hutchcroft, L. Iacobuzi, E. Iacopini, E. Imbergamo, B. Jenninger, J. Jerhot, R.W. Jones, K. Kampf, V. Kekelidze, S. Kholodenko, G. Khorauli, A. Khotyantsev, A. Kleimenova, A. Korotkova, M. Koval, V. Kozhuharov, Z. Kucerova, Y. Kudenko, J. Kunze, V. Kurochka, V. Kurshetsov, G. Lanfranchi, G. Lamanna, E. Lari, G. Latino, P. Laycock, C. Lazzeroni, M. Lenti, G. Lehmann Miotto, E. Leonardi, P. Lichard, L. Litov, R. Lollini, D. Lomidze, A. Lonardo, P. Lubrano, M. Lupi, N. Lurkin, D. Madigozhin, I. Mannelli, G. Mannocchi, A. Mapelli, F. Marchetto, R. Marchevski, S. Martellotti, P. Massarotti, K. Massri, E. Maurice, M. Medvedeva, A. Mefodev, E. Menichetti, E. Migliore, E. Minucci, M. Mirra, M. Mishaeva, N. Molokanova, M. Moulson, S. Movchan, M. Napolitano, I. Neri, F. Newson, A. Norton, M. Noy, T. Numao, V. Obraztsov, A. Ostankov, S. Padolski, R. Page, V. Palladino, A. Parenti, C. Parkinson, E. Pedreschi, M. Pepe, M. Perrin-Terrin, L. Peruzzo, P. Petrov, Y. Petrov, F. Petrucci, R. Piandani, M. Piccini, J. Pinzino, I. Polenkevich, L. Pontisso, Yu. Potrebenikov, D. Protopopescu, M. Raggi, A. Romano, P. Rubin, G. Ruggiero, V. Ryjov, A. Salamon, C. Santoni, G. Saracino, F. Sargeni, S. Schuchmann, V. Semenov, A. Sergi, A. Shaikhiev, S. Shkarovskiy, D. Soldi, V. Sugonyaev, M. Sozzi, T. Spadaro, F. Spinella, A. Sturgess, J. Swallow, S. Trilov, P. Valente, B. Velghe, S. Venditti, P. Vicini, R. Volpe, M. Vormstein, H. Wahl, R. Wanke, B. Wrona, O. Yushchenko, M. Zamkovsky, A. Zinchenko.

1. Introduction

Several models aimed at explaining the dominance of dark matter on ordinary matter in the Universe have been proposed. One of the possible models answering to this question introduces an extra U(1) gauge-symmetry with a corresponding new massive vector mediator field A' , called *dark photon*. The simplest realization of this model assumes that the A' field interacts with the SM photon via a kinetic mixing term [2]:

$$\mathcal{L}_{mix} = \varepsilon A'_{\mu\nu} F^{\mu\nu} \quad (1.1)$$

where $F^{\mu\nu}$ represents the electromagnetic field and $\varepsilon \ll 1$ is the coupling parameter. Further interactions with both SM fields and hidden sectors fields are also possible. If these are lighter than the A' , then the dark photon would decay mostly in invisible. The dominant production mechanism for the A' depends on the mass of the hidden sector portal. If $M_{A'} < M_{\pi^0}$ the dominant production mechanism is

$$\pi^0 \rightarrow A' \gamma \quad (1.2)$$

with a branching ratio which depends on the mass of the new hidden particle as shown in (1.3).

$$Br(\pi^0 \rightarrow A' \gamma) = 2\varepsilon^2 \left(1 - \frac{M_{A'}^2}{M_{\pi^0}^2}\right)^3 \times Br(\pi^0 \rightarrow \gamma\gamma) \quad (1.3)$$

The search for an invisible A' at NA62 is performed with a peak searching in the missing-mass distribution technique by means of the full reconstruction of the decay chain

$$K^+ \rightarrow \pi^+ \pi^0, \pi^0 \rightarrow A' \gamma \quad (1.4)$$

2. The NA62 experiment

The NA62 experiment is a fixed target experiment located at CERN. The main goal of NA62 is to measure the branching ratio of the ultra rare decay $K^+ \rightarrow \pi^+ \nu \bar{\nu}$ with a 10% precision using a decay-in-flight technique [3]. To reach the desired performance the NA62 experiment aims to collect a large number ($O(10^{13})$) of kaon decays in a 50 m decay volume and assuming that 10% of the kaons produced decay, a rejection factor of $O(10^{12})$ is required. The experiment was designed in order to guarantee high intensity, full particle identification, hermetic coverage, low material budget and high-rate tracking.

The schematic of the beam line and detector is shown in Figure 1. The NA62 beam is an unseparated beam of positive particles, produced by the interaction of the 400 GeV/c protons from the Super Proton Synchrotron (SPS) with a Beryllium target. The beam is composed of protons (23%), pions (70%) and kaons (6%) with an average momentum of 75 GeV/c and a 1% RMS momentum bite. The secondary beam produced is then collimated and directed through the detector. Before enter the decay region kaons are positively identified by a differential Cherenkov counter with 70 ps time resolution while momentum and directions of all incoming particles are measured with a hybrid Si-pixel detector, GigaTracker (GTK) composed of 3 stations displaced around an achromat, with a time resolution of 100 ps, a longitudinal momentum resolution of 0.15 GeV/c

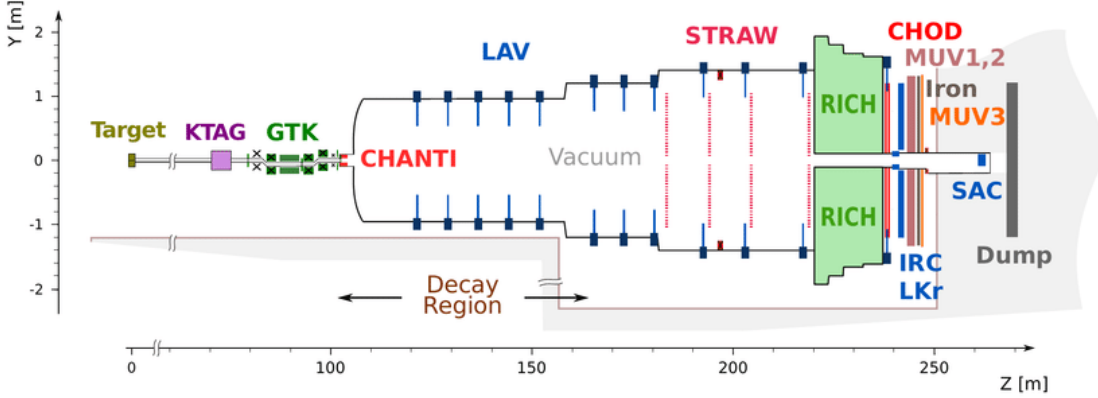


Figure 1: Schematic top view of the NA62 beam line and detector.

and an angular resolution of $16 \mu\text{rad}$. The beam enters a vacuum (10^{-6} mbar) cylindrical tank and decays in a 50 m long region. The momentum and position of charged daughter particles are measured by a spectrometer consisting of two straw-tube chambers (STRAW) on either side of a dipole magnet providing a transverse horizontal momentum kick of $270 \text{ MeV}/c$. The spectrometer momentum resolution σ_P/P is in the range of 0.3-0.4%. Secondary charged pions are identified by a ring-imaging Cherenkov detector (RICH) with 70 ps time resolutions: it is built in such a way that in the relevant track momentum range $[15,35] \text{ GeV}/c$, the probability of π^+/μ^+ mis-identification is smaller than 1%. Daughter photons are detected by a hermetic system involving several detectors: two lead-scintillator calorimeters (IRC and SAC) for emission angles with respect to the Z axis $\theta < 1 \text{ mrad}$, a liquid krypton electromagnetic calorimeter (LKr) for $1 < \theta < 10 \text{ mrad}$, and a system of 12 annular lead-glass detectors (LAV) for $10 < \theta < 50 \text{ mrad}$. The detection inefficiency for IRC and SAC is of 10^{-3} for photons with energy above 6 GeV, for LKr is of 10^{-5} for photons with energy above 10 GeV and for LAV is of 10^{-3} for photons with energy above 1 GeV. The LKr provides measurements of the energy, transverse positions, and time with resolutions of $\sigma_E/E = 4.8\%/\sqrt{E[\text{GeV}]} \oplus 11\%/E[\text{GeV}] \oplus 0.9\%$, 1 mm, and 500 ps respectively. Two charged hodoscope, CHOD and NA48-CHOD, are placed after the spectrometer, providing fast time response for charged particles. Two hadronic iron/scintillator-strip sampling calorimeters (MUV1,2) and an array of scintillator tiles located behind 80 cm of iron (MUV3) supplement the pion/muon identification system. The overall probability for identifying a μ^+ as a π^+ in the momentum range 15-35 GeV/c is at the level of 10^{-7} [4, 5].

Information from the NA48-CHOD, CHOD, RICH, MUV3, LKr, and the most downstream LAV station (LAV12) is hardware-processed to issue level-zero (L0) trigger signals with a frequency up to 1 MHz. A software trigger (L1) reconstructs data from the KTAG, LAV and STRAW to further enforce the signals selection with a frequency up to 10 KHz [6].

3. The analysis

The experimental signature to search for an invisible A' as described in (1.4) is given by a kaon decaying into a charged pion and a photon hitting the LKr calorimeter, with missing energy and

momentum. The squared missing mass is defined as

$$M_{miss}^2 = (P_K - P_\pi - P_\gamma)^2 \quad (3.1)$$

where P_K and P_π denotes the kaon and pion 4-momentum measured with GTK and STRAW, respectively and P_γ is the the photon 4-momentum determined from the measure of the photon position of impact and energy deposition in the LKr, assuming emission from the decay vertex. The M_{miss}^2 is expected to peak at $M_{A'}^2$ for the decay chain in (1.4) and at zero for the most abundant background, $\pi^0 \rightarrow \gamma\gamma$ with one photon undetected.

The data sample used for this analysis has been collected by a L0 trigger condition which aims to select final states with one emitted π^+ and missing energy. The number of tagged π^0 mesons for normalization (n_{π^0}) is computed selecting $K^+ \rightarrow \pi^+\pi^0$ from data taken with a minimum-bias L0 trigger ("control trigger") downscaled by a factor of 400. The $K^+ \rightarrow \pi^+\pi^0$ events selection is based on the reconstruction of K^+ and π^+ tracks and on the squared missing mass kinematic variable, cutting around the π^0 mass peak. These requests are applied also for the signal selection, together with more strict conditions to enforce the presence of a single π^+ and of a single photon on the LKr. The number of tagged π^0 mesons in the sample analyzed is $n_{\pi^0} = 4.12 \times 10^8$.

An illustration of the expected distribution of the M_{miss}^2 for the signal using Monte Carlo samples and for the most abundant background using the control-trigger data sample with fully reconstructed $\pi^0 \rightarrow \gamma\gamma$ in which one of the two photon LKr clusters, randomly chosen, is artificially excluded is shown in Figure 2. The data distribution, in blue, is scaled to the number of tagged π^0 , counted in the control-trigger while each MC distribution is scaled to the equivalent number of tagged π^0 corresponding to the generated statistics.

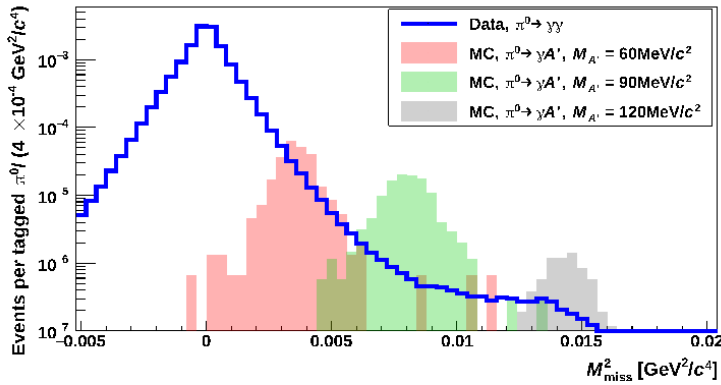


Figure 2: Distributions of M_{miss}^2 evaluated from K^+ decays with one photon and one π^+ reconstructed. The blue line shows data from $\pi^0 \rightarrow \gamma\gamma$ with one photon, randomly chosen, assumed to be undetected. The filled histograms represent the expected distribution for signal events from a MC simulation assuming three A' mass hypothesis, 60, 90 and 120 MeV/c^2 and a coupling strength $\epsilon^2 = 2.5 \times 10^{-4}$.

As said before, the most abundant background is represented by the $K^+ \rightarrow \pi^+\pi^0$, $\pi^0 \rightarrow \gamma\gamma$ decay chain, where one photon is lost due to photo-nuclear interaction or conversions downstream of the NA48-CHOD. The expected background has been evaluated using a data-driven approach. In order to have a sample populated of $\pi^0 \rightarrow \gamma\gamma$ with one photon lost, the same selection for the

signal but the cut on the NA48-CHOD extra activity¹ is applied. This selection ensure the presence of a second photon with no overlap with the signal sample. This control sample is scaled to the signal sample in a side-band region adjacent to but not overlapping with the A' search region. The distributions of M_{miss}^2 for the signal search and the scaled background are shown in Figure 3.

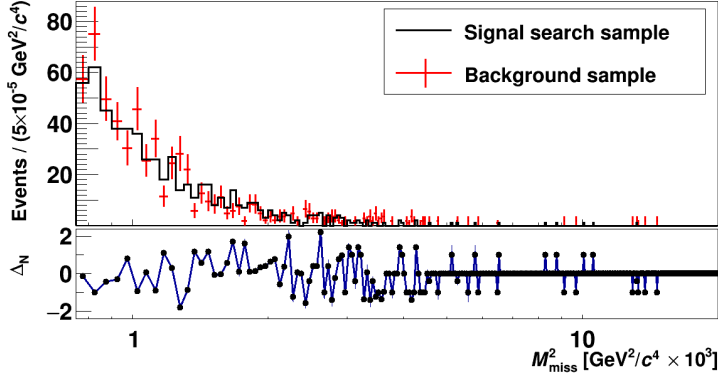


Figure 3: M_{miss}^2 distribution in the search region $[0.00075, 0.01765] \text{ MeV}^2/c^4$ for signal (black) and background (red). In the bottom panel, the difference Δ_N between the two M_{miss}^2 spectra in units of its standard deviation is shown.

For the A' search, background considerations suggest considering a minimum mass of $30 \text{ MeV}/c^2$, while acceptance and yield consideration suggest considering a maximum mass of $130 \text{ MeV}/c^2$.

The expected branching ratio for the decay under study can be express in terms of the number of signal events n_{sig} in the given M_{miss}^2 window normalized to the number of tagged π^0

$$Br(\pi^0 \rightarrow A' \gamma) = Br(\pi^0 \rightarrow \gamma \gamma) \frac{n_{sig}}{n_{\pi^0}} \frac{1}{\epsilon_{sel} \epsilon_{trg} \epsilon_{mass}} \quad (3.2)$$

where ϵ_{sel} and ϵ_{trg} , represent the signal selection efficiency and the signal-trigger efficiency, respectively depending on the A' mass, while ϵ_{mass} account for the acceptance of the sliding M_{miss}^2 window used. The total efficiency as a function of $M_{A'}$, evaluated using MC simulations, is shown in Figure 4.

A peak search in the positive tail of the M_{miss}^2 background distribution is performed by comparing the number of events in a sliding M_{miss}^2 window to the background expectation. Given the expected background, for each A' mass value the signal region optimizing the upper limit in a background-only hypothesis is defined as a $\pm 1\sigma_{M_{miss}^2}$ window around the expected M_{miss}^2 peak value, where $\sigma_{M_{miss}^2}$ is the squared missing mass resolution.

4. Results

Using the CLs algorithm, 90% CL upper limits on the coupling parameter ϵ^2 as a function of $M_{A'}$ have been set. The upper limits are compatible within two standard deviations with the

¹No in-time NA48-CHOD candidates must be found except for those geometrically associated with the π^+

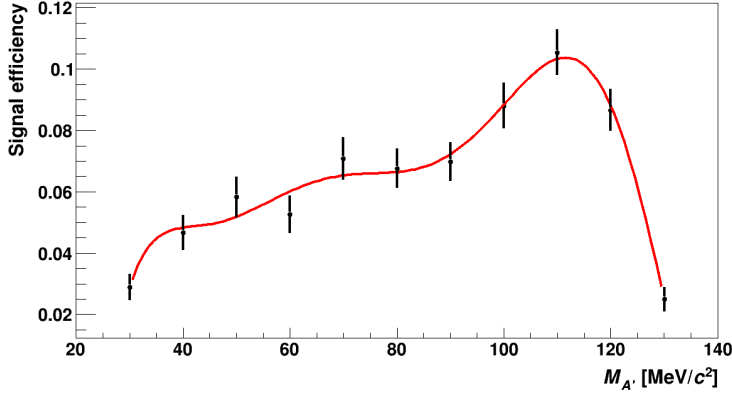


Figure 4: Total signal efficiency as a function of the A' mass hypothesis in the 30-130 MeV/c^2 region. A polynomial is used to interpolate the global efficiency

fluctuation expected in a background-only scenario as shown in Figure 5. The statistical treatment takes into account the systematic uncertainty evaluated varying the parameters used in the statistical procedure (the scale factors mass window and the signal mass window). The uncertainties on the signal efficiency, including statistical and systematic errors, have been also considered in the evaluation of the upper limit.

With few changes in the analysis a search for $\pi^0 \rightarrow \gamma \nu \bar{\nu}$ has been performed. A new limit on the branching ratio at 90% CL has been set

$$Br(\pi^0 \rightarrow \gamma \nu \bar{\nu}) < 1.9 \times 10^{-7} \quad (4.1)$$

improving by more than three order of magnitude with respect to the present limit [7].

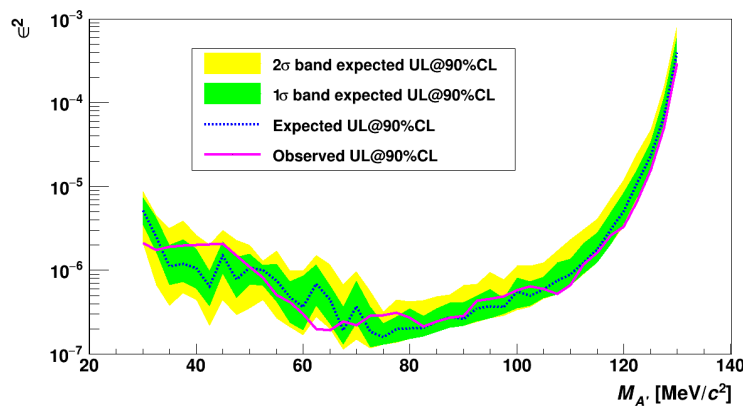


Figure 5: The 90% CL upper limits on the coupling parameter ϵ^2 as a function of $M_{A'}$. The limit obtained from data (solid line) and the limit expected in the absence of signal (dashed line) are shown.

5. Conclusions

A search for an invisible dark photon A' at NA62 has been presented. No statistically significant excess is detected and upper limits on the coupling parameter ε^2 in the mass range 30-130 MeV/ c^2 have been set, improving on previous results in the mass range 60-110 MeV/ c^2 (Figure 6). The analysis has been performed on a sub-sample corresponding to only 1% of the full statistics available. From the analysis of the full statistics further improvements are expected.

The experimental technique illustrated here differs from that of previous experiments. Processes involving suppressed dark-photon lepton coupling might produce a signal in NA62, while experiments as BaBar [8] or NA64 [9] cannot be sensitive to such processes as they use electron/positron beams.

Finally a stringent limit on the $\pi^0 \rightarrow \gamma\nu\bar{\nu}$ has been set improving on previous results by more than three order of magnitude.

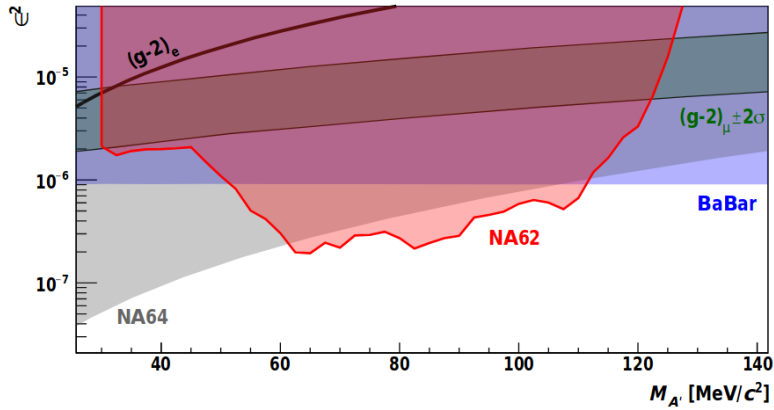


Figure 6: Upper limit at 90% CL from NA62 (red region) in the ε^2 vs $M_{A'}$ plane with A' decaying into invisible final states. The limits from the BaBar[8] (blue) and NA64 [9] (light grey) experiments are shown.

References

- [1] E.Cortina Gil, et al. [The NA62 Collaboration] J. High Energ. Phys. (2019) 182
- [2] B. Holdom, Phys. Lett. B 166 (1986) 196
- [3] A. J. Buras, D. Buttazzo, J. Girrbach-Noe and R. Knegjens, JHEP 1511 (2015) 033
- [4] E. Cortina Gil, et al. [The NA62 Collaboration], J. Instrum. 12 (2017) P05025
- [5] E. Cortina Gil, et al. [The NA62 Collaboration], Phys. Lett. B 791 (2019) 156
- [6] R. Ammendola, et al. Nucl.Instrum.Meth. A929 (2019) 1-22
- [7] M. S. Atiya, et al. [The E787 Collaboration], Phys. Rev. Lett. 69 (1992) 733
- [8] J. P. Lees, et al. [The BaBar Collaboration], Phys. Rev. Lett. 119 (2017) 131804
- [9] D. Banerjee, et al. [The NA64 Collaboration] Phys. Rev. D 97 (2018) 072002